

Article ID: 1006-8775(2012) 02-0187-08

ON THE RELATIONSHIPS BETWEEN THE UNUSUAL TRACK OF TYPHOON MORAKOT (0908) AND THE UPPER WESTERLY TROUGH

FEI Jian-fang (费建芳), LI Bo (李 波), HUANG Xiao-gang (黄小刚), CHENG Xiao-ping (程小平)

(Institute of Meteorology, PLA University of Science and Technology, Nanjing 211101 China)

Abstract: In this paper, by carrying out sensitivity tests of initial conditions and diagnostic analysis of physical fields, the impact factors and the physical mechanism of the unusual track of Morakot in the Taiwan Strait are discussed and examined based on the potential vorticity (PV) inversion. The diagnostic results of NCEP data showed that Morakot's track was mainly steered by the subtropical high. The breaking of a high-pressure zone was the main cause for the northward turn of Morakot. A sensitivity test of initial conditions showed that the existence of upper-level trough was the leading factor for the breaking of the high-pressure zone. When the intensity was strengthened of the upper-level trough at initial time, the high-pressure zone would break ahead of time, leading to the early northward turn of Morakot. Conversely, when the intensity was weakened, the breaking of the high-pressure zone would be delayed. Especially, when the intensity was weakened to a certain extent, the high-pressure zone would not break. The typhoon, steered by the easterly flow to the south of the high-pressure zone, would keep moving westward, with no turn in the test. The diagnostic analysis of the physical fields based on the sensitivity test revealed that positive vorticity advection and cold advection associated with the upper-level trough weakened the intensity of the high-pressure zone. The upper-level trough affected typhoon's track indirectly by influencing the high-pressure zone.

Key words: typhoon; unusual track; potential vorticity (PV) inversion; upper-level trough

CLC number: P444

Document code: A

doi: 10.3969/j.issn.1006-8775.2012.02.008

1 INTRODUCTION

Typhoon track is an important part of typhoon research. The accuracy of numerical prediction about typhoon track has been improved significantly in recent years, though the forecast ability for a few unusual typhoons remains very low, which is currently one of the three unresolved problems in typhoon study over the world^[1]. The breaking of a high-pressure zone is found to be the main cause for the northward turn of Helen (9505) (Zhang et al.^[2]). Fan et al.^[3] concluded that two significant eastward turnings of Matsa (0509) had close relationship with the adjusting of the westerly circulation. According to the statistical analysis of the observations, the movement of Northwest Pacific typhoon is closely related to the upper-flow of Qinghai-Tibet Plateau (Xu et al.^[4]).

In this paper, Typhoon Morakot (0908) is studied by combining diagnostic analysis and numerical simulation based on the inversion of potential

vorticity (PV). By carrying out sensitivity tests of initial conditions and diagnostic analysis of physical fields, the impact factors and the physical mechanism of the unusual track of Morakot in the Taiwan Strait are discussed and examined.

The paper is organized as follows. The datasets and methodology are described in section 2, the results of global analysis data are studied in detail in section 3, followed by further discussion of the results of numerical simulation in section 4. Main conclusions and discussion are summarized in section 5.

2 ANALYSIS METHODS AND EXPERIMENTAL DESIGN

The best-track dataset for tropical cyclones in the western North Pacific is from China Meteorological Administration / Shanghai Typhoon Institute (CMA-STI). The data used in this study are from the U.S. National Centers for Environmental

Received 2011-09-30; **Revised** 2012-02-15; **Accepted** 2012-04-15

Foundation item: National Public Benefit (Meteorology) Research Foundation of China (GYHY201106004); National Basic Research Program "973" of China (2009CB421502); National Nature Science Foundation of China (40730948, 41005029)

Biography: FEI Jian-fang, Professor, primarily undertaking the research on the mesoscale meteorology.

Corresponding author: FEI Jian-fang, e-mail: feijf@sina.com

Prediction/National Center for Atmospheric Research (NCEP/NCAR) reanalysis dataset, which has a horizontal resolution of $1^\circ \times 1^\circ$, and 26 vertical layers on standard pressure surfaces.

2.1 Methods

The use of PV for understanding the evolution of the dynamical system in the atmosphere has been well reviewed in Hoskins et al.^[5]. Such merit is particularly enhanced with its inversion characteristics. The PV invertibility principle states that given a distribution of PV, a prescribed balanced condition and boundary conditions, balanced mass and wind fields can be recovered. The Ertel potential vorticity inversion has been widely used in many areas of typhoon research since Davis and Emanuel^[6] proposed a piecewise PV inversion in 1991^[7-14].

Based on the piecewise PV inversion principle (Davis and Emanuel^[6], Wang and Zhang^[13]), we can complete the techniques in such specific steps as follows: (1) mean fields: the mean field of streamfunction and the geopotential height are determined by taking time averages, and the mean field of PV is calculated using the approximate definition of Ertel's PV; (2) entire perturbation field: it is obtained by making subtraction between the actual field and the mean field; (3) specific

perturbation field: spatial distribution of the specific weather systems in the geopotential height field are compared, and specific perturbation fields associated with specific weather systems in the whole perturbation field are separated. (4) balanced field: the three-dimensional geopotential height, stream function, wind and temperature fields associated with specific PV perturbation are derived by performing piecewise PV inversion; (5) specific application: the balanced field is applied to specific issues of typhoon research by combining diagnostic analysis or numerical simulation.

The steering flow of each storm is defined as a deep-layer-mean wind vector averaged over the inner $7^\circ \times 7^\circ$ around the storm's center (based on the location of the minimum sea level pressure).

According to the work of Arthur^[15], the deep-layer-mean can be calculated as follows:

$$U = (75U_{1000} + 150U_{850} + 175U_{700} + 150U_{500} + 100U_{400} + 75U_{300} + 50U_{250} + 50U_{200} + 50U_{150} + 25U_{100})/900$$

where U represents velocity component on the x coordinate corresponding to a particular isobaric surface. The calculation of V is similar with that of U . Different typhoon central pressures correspond to different layers of the steering flow (Table 1).

Table 1. Minimum sea level pressure and corresponding steering layer.^[16]

Minimum sea level pressure P(hPa)	$P \geq 990$	$970 \leq P < 990$	$950 \leq P < 970$	$940 \leq P < 950$	$P < 940$
Steering layer (hPa)	500–850	400–850	300–850	250–850	200–700

2.2 Experimental design

A series of sensitivity experiments are conducted to explore the factors controlling the movement of Morakot. The point (125°E , 30°N) is chosen to be the center of the simulated area. The model configuration includes single grids, with horizontal resolutions of 30 km, and $214 \times 161 \times 27$ grids. The initial and boundary conditions are taken from NCEP $1^\circ \times 1^\circ$ global reanalysis data. Each simulation is integrated for 72 h, starting from 0600 UTC 6 August 2009.

Based on the control experiment, the upper-level trough's intensity of different sensitivity experiments is calculated by the following formula:

$$New_Trough = Ctr_Trough + Pv_Trough \times S1$$

where the *New_Trough* represents the initial intensity of the upper-level trough in the sensitivity experiment, the *Ctr_Trough* represents the intensity of the upper-level trough of the control experiment at the initial time, and the *Pv_Trough* represents the three-dimensional balanced fields of (temperature,

wind, geopotential height) inverted by the PV perturbation associated with the upper-level trough, $S1$ indicates the strength factor of the sensitivity experiment. When $S1$ is equal to 0, it means there is no change in the upper-level trough. When $S1$ is larger than 0, it means the upper-level trough is strengthening. When $S1$ is smaller than 0, it means the intensity is weakening. In this paper, $S1$ is set from -1 to 0.5 , with an interval of 0.05 , and a total of 30 sensitivity experiments are designed.

3 RESULTS OF GLOBAL ANALYSIS DATA

3.1 Synopsis

Morakot (0908) is a typhoon which moves in the eastern coast and has a significant impact on China in August 2009. Morakot formed in the evening of 3 August over the Northwest Pacific before moving westward, with its intensity gradually increased. As shown in Figure 1, Morakot landed on the coastal areas of Taiwan at 1500 UTC 7 August. At 1200 UTC

8 August, the track of Morakot curved rather sharply towards the north after moving into the Taiwan Strait. Morakot kept moving northward and made its final landfall on Fujian province.

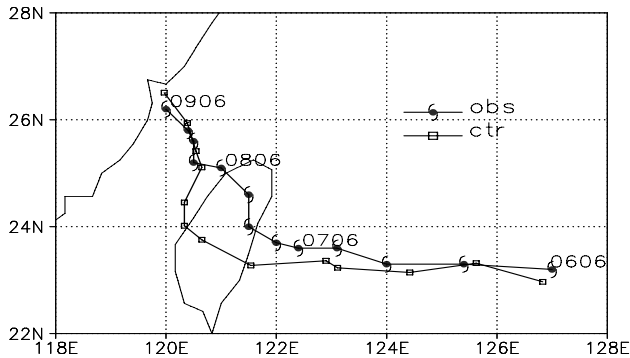


Figure 1. CMA-STI best track and the simulated typhoon track from 0600 UTC 6 August to 0600 UTC 9 August 2009.

3.2 PV diagnosis

According to the evolution of the geopotential

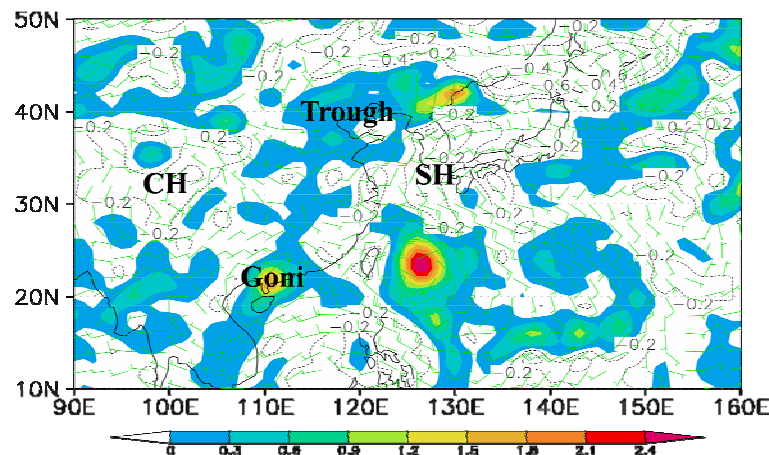


Figure 2. Potential vorticity perturbation (contour interval of 0.2 PVU; the area with positive PV value is shaded) and wind (one full wind barb 4 m/s) at 500 hPa at 0600 UTC 6 August 2009.

Following Wu et al.^[9], to evaluate the steering flow due to various PV perturbations, the time series of the deep-layer-mean steering flows (Figure 3) associated with each PV perturbation [$V_m(\text{SH}_{\text{pv}})$], $V_m(\text{Goni}_{\text{PV}})$, [$V_m(\text{CH}_{\text{PV}})$], [$V_m(\text{Trough}_{\text{pv}})$], and [$V_m(\text{CH}_{\text{PV}})$]] were compared with the actual movement of Morakot [$V(\text{Morakot})$](estimated from the 12-h best-track positions).

As shown in Figure 3, the deep-layer-mean steering flow associated with the subtropical high made the greatest contribution to the actual movement of Morakot, with its track mainly steered by the subtropical high. The contributions of the other three dynamical systems were relatively small, with little direct impact on Morakot's movement.

height field at 500 hPa from 1200 UTC 7 August to 1800 UTC 8 August 2009, there were four main synoptic weather systems around Morakot during its period of unusual track. To show how the different dynamical systems affect the movement of Morakot, the piecewise PV inversion was performed following the approach of Davis and Emanuel^[6], Wang and Zhang^[13]. The piecewise PV inversion was performed to calculate the balanced flow and mass field associated with each of the PV perturbations.

An example time (0600 UTC 6 August) was chosen to show the PV perturbation field (Figure 2), with the whole PV perturbation divided into several parts, i.e., SH, CH, Trough, and Goni, representing the PV perturbation associated with the subtropical high, the continental high, the upper-level trough, and typhoon Goni, respectively. The flow field that was attributed to different PV perturbation and the steering flow attributed to different dynamical systems were calculated.

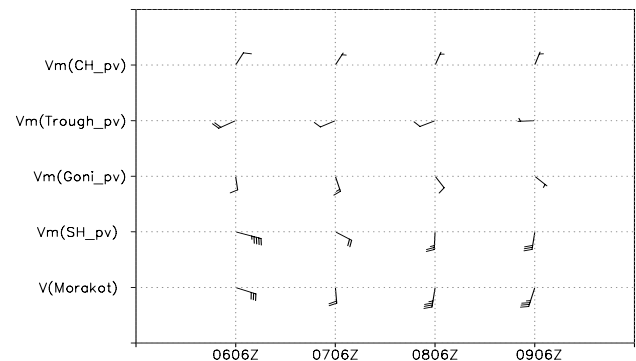


Figure 3. Time series of Morakot's movement ($V(\text{Morakot})$) and the steering flow associated with the subtropical high PV perturbation [$V_m(\text{SH}_{\text{pv}})$], the Goni PV perturbation [$V_m(\text{Goni}_{\text{PV}})$], the Continental high PV perturbation [$V_m(\text{CH}_{\text{PV}})$], and the upper-level trough PV perturbation [$V_m(\text{Trough}_{\text{pv}})$] from 0600 UTC 6 August to 0600 UTC 9 August 2009 (every 24 hours). One full barb is 1 m/s.

3.3 Situation analysis

As shown in the evolution of the geopotential height field at 300 hPa from 1200 UTC 7 August to 1800 UTC 8 August 2009, the subtropical high and the continental high were both located over the same high-pressure zone (indicated by the isobaric line of 9720 geopotential meters). With the high-pressure zone gradually weakening and breaking up, Morakot gradually moved northwest (Figure 1). Morakot made a sudden turning to the north after a short time of westward movement from 0600 UTC 8 August to 1200 UTC 8 August. At the same time, the zonal high-pressure zone broke into two high-pressure

systems, enclosed and massive. From then on, Morakot kept moving northward in the southerly flow to the rear of the subtropical high.

The evolution of the average geopotential height field of the whole layer is shown in Figure 4. It indicates that the western ridge of the subtropical high remained at 117°E before 1200 UTC 7 August. As the high-pressure gradually weakened, the western ridge moved eastward to 122°E at 1800 UTC 7 August and remained there for a long time until 1200 UTC 8 August. Then the western ridge of the high-pressure suddenly jumped eastwards from 122°E to 130°E from 1200 to 1800 UTC 8 August while Morakot turned northward.

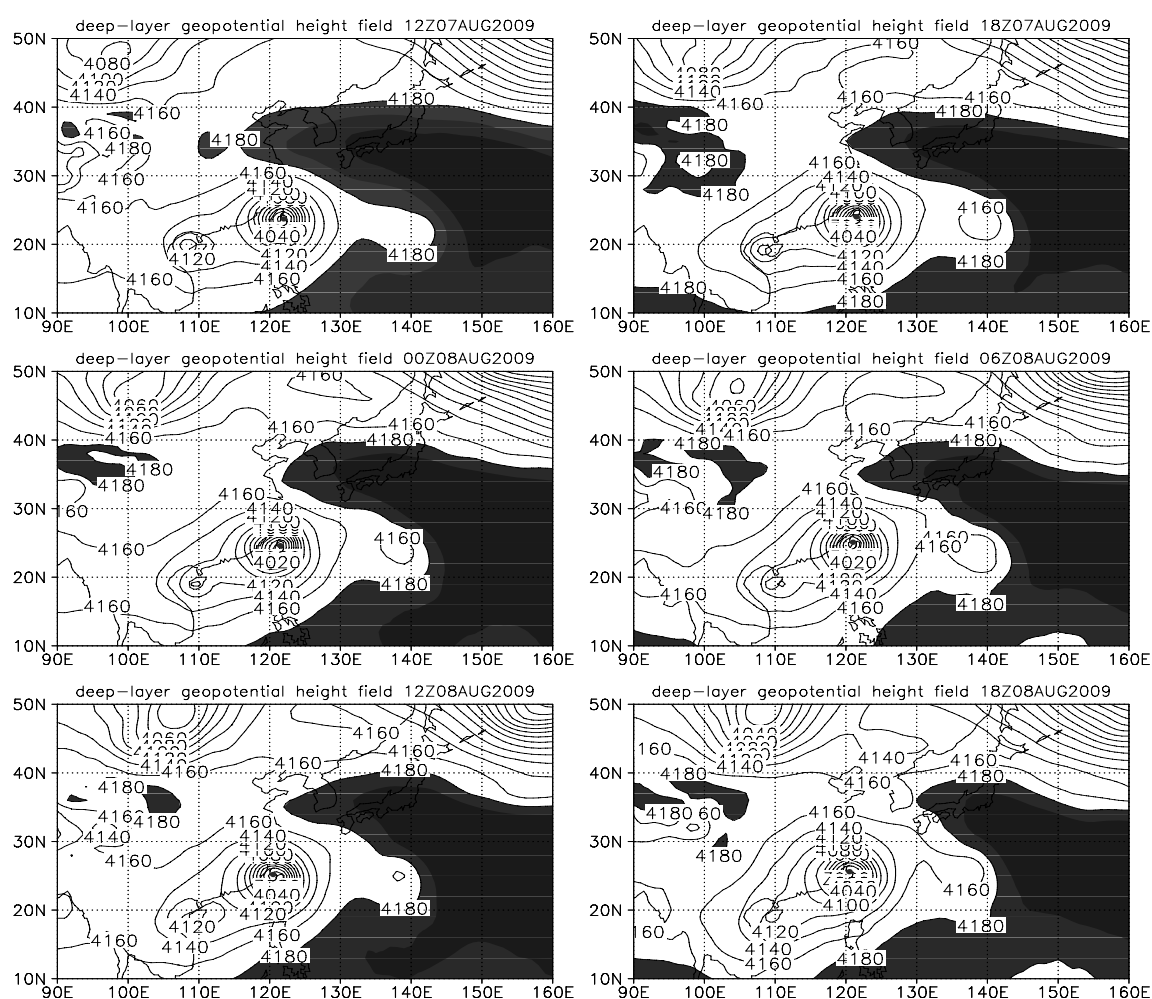


Figure 4. Deep-layer mean geopotential height (contour interval of 20 gpm; the area with values larger than 4180 gpm is shaded) from 1200 UTC 7 August to 1800 UTC 8 August 2009.

It is concluded from the above analysis that Morakot's track was mainly steered by the subtropical high, with the split of the high-pressure zone as the main reason for the northward turning of Morakot.

3.4 Average vorticity analysis

It is shown from the above analysis that the upper-level trough was mainly in the upper

troposphere (250 hPa) and Morakot was in the mid- and upper-level (600 hPa). The evolution (shown in Figure 5) of the vorticity fields, which were respectively averaged over 30° to 42°N at 300 hPa, 19° to 28°N at 500 hPa, and the variation of the western ridge point, which are referred to as the west longitude of the deep-layer mean geopotential height, clearly illustrated the relationships among the split of the high-pressure zone, the upper-level trough and

Morakot.

As shown in Figure 5, the western ridge of the high-pressure experienced two distinct processes of withdrawal. Coincided with the evolution of the vorticity associated with the upper-level trough, the intensity of the upper-level trough strengthened in the process of eastward withdrawal before 1200 UTC 7 August. The upper-level trough kept transporting positive vorticity into the high-pressure zone, reducing its intensity, and leading to the first withdrawal of the western ridge. Coincided with the evolution of the vorticity associated with Morakot, the

intensity of the upper-level trough weakened after 1200 UTC 7 August while Morakot moved westward, with both systems transporting positive vorticity into the high-pressure zone. At 0600 UTC 8 August, the vorticity fields of the upper-level trough and Morakot moved toward each other at around 120°E at the same longitude. The combined effects of the two led to a significant weakening of the high-pressure zone. At 0600 UTC 8 August, the high-pressure zone was cut off, and the western ridge withdrew eastward, resulting in the northward turning of Morakot.

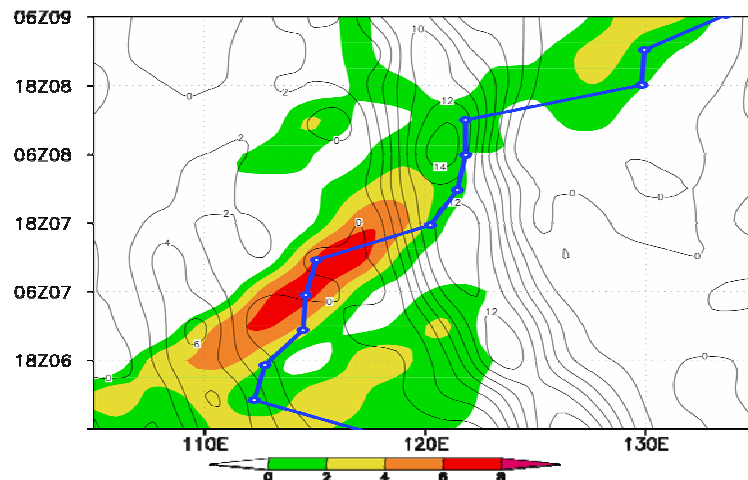


Figure 5. The longitude-time cross section for the vorticity (10^{-5} s^{-1}) averaged over 30–42°N (shadings) at 300 hPa and over 19–28°N (solid line) at 500 hPa, and the longitude position of the deep-layer mean geopotential height (dash line) from 0600 UTC 6 August to 0600 UTC 9 August 2009.

4 RESULTS OF NUMERICAL SIMULATION

4.1 Control experiment

As the WRF mesoscale model simulated the northward turning of Morakot reasonably well (as shown in Figure 1), this is made to be a control test for the sensitivity testing of initial conditions.

4.2 Sensitivity study

The tracks of Morakot in each sensitivity experiment are shown in Figure 6. When the strength factor S1 gradually increased from 0.05 to 0.5, Morakot turned northward ahead of time. When S1 gradually decreased from -0.05 to -1 , Morakot gradually moved more southward, and the trend of turning became increasingly insignificant. When S1 decreased to -0.9 , Morakot kept moving westward without turning.

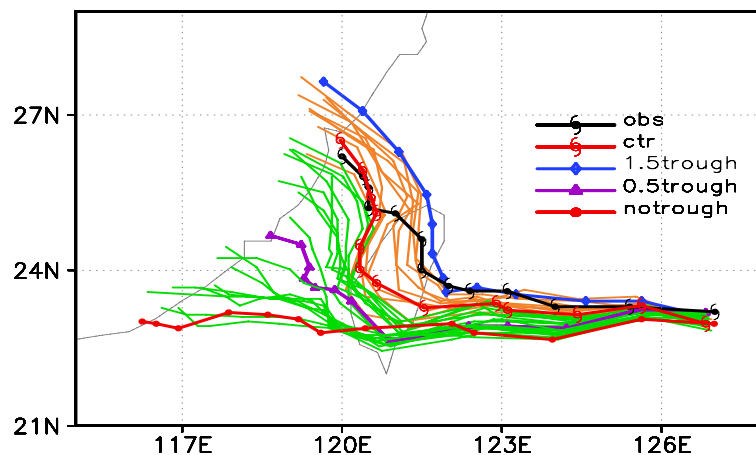


Figure 6. Model tracks of all sensitivity experiments at 6-h intervals from 0600 UTC 6 August to 0600 UTC 9 August 2009.

Although an upper-level trough was far away from Morakot in the model initial time, the intensity change of the upper-level trough had an important influence on the movement of Morakot during the next 72 hours. With different intensity, the upper-level trough played different roles in weakening the intensity of the high-pressure zone, resulting in different situations of the high-pressure zone and different tracks of Morakot in the experiment.

4.3 Mechanism analysis

Figure 7 shows the longitude-time cross sections for the vorticity averaged over 30–42°N (shadings) at 300 hPa in the control test, 1.5 trough test, 0.5 trough test and no-trough test. Clearly, both the scope and

size of the vorticity associated with the upper-level trough in the initial time in the 1.5 trough test were bigger than those in the control test. In the 0.5 trough test and no-trough test, the corresponding scope and size of the vorticity were smaller than those in the control test. With strengthened intensity of the upper-level trough in the initial time, the accumulation and transport of the vorticity associated with the upper-level trough into the high-pressure zone became stronger, and the high-pressure zone broke ahead of time, leading to early northward turning of Morakot. Conversely, the rupture of the high-pressure zone would be delayed, especially in the no-trough test in which the high-pressure zone would not break.

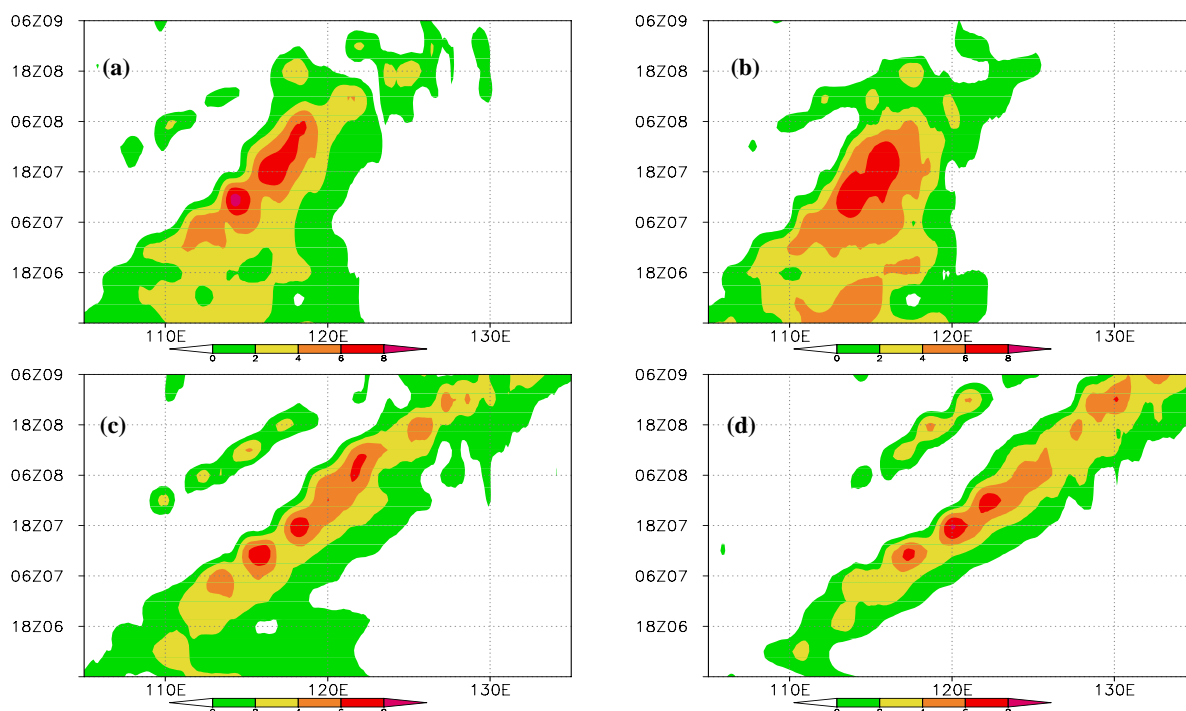


Figure 7. The longitude-time cross section for the vorticity (10^{-5} s^{-1}) averaged over 30–42°N (shadings) at 300 hPa from 0600 UTC 6 August to 0600 UTC 9 August 2009. (a) control test, (b) 1.5 trough test, (c) 0.5 trough test, (d) no-trough test.

The longitude-time cross sections for the temperature advection averaged over 30–42°N (shadings) at 300 hPa in the control test, 1.5 trough test, 0.5 trough test and no-trough test are displayed in Figure 8. Similarly, the cold advection associated with the upper-level trough continuously delivered cold air into the high-pressure zone, reducing its intensity.

When the intensity of the upper-level trough strengthens in the initial time, the cold advection associated with the upper-level trough into the high-pressure zone became stronger. Conversely, with $S1$ decreased from -0.25 to -1 , the rupture of the high-pressure zone would delay, especially in the

no-trough test in which the high-pressure zone would not break. With the intensity factor $S1$ decreased from 0 to -1 , both the scope and size of the cold advection associated with the upper-level trough in the initial time became smaller, and the accumulation transport also became smaller.

The analysis results above imply that the upper-level trough was the main system leading to the split of the high-pressure zone. With the upper-level trough moving eastward and southward, both the vorticity and the cold advection associated with the upper-level trough would reduce the intensity of the high-pressure zone.

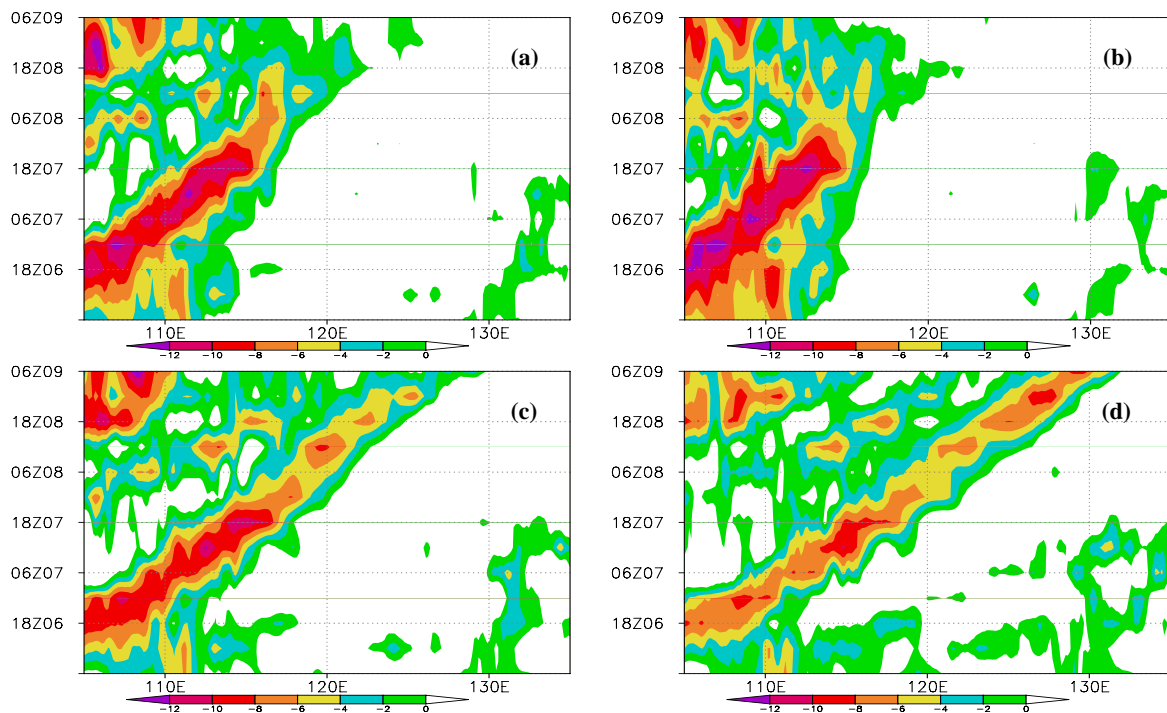


Figure 8. The longitude-time cross section for the temperature advection (10^{-5} K/s) averaged over $30\text{--}42^{\circ}\text{N}$ (shadings) at 300 hPa from 0600 UTC 6 August to 0600 UTC 9 August 2009. (a) control test, (b) 1.5 trough test, (c) 0.5 trough test, (d) no-trough test.

5 SUMMARY

In this paper, typhoon Morakot (0908) is studied by combining diagnostic analysis and numerical simulation based on the PV inversion. By carrying out sensitivity tests of initial conditions and diagnostic analysis of physical fields, the impact factors and the physical mechanism of the unusual track of Morakot in the Taiwan Strait are discussed and examined. Based on the foregoing analysis, the following conclusions are obtained:

(1) The diagnostic results of NCEP data showed that Morakot's track was mainly steered by the subtropical high, and the breaking of the high-pressure zone was the main cause for the northward turning of Morakot.

(2) The WRF mesoscale model simulated the northward turning of Morakot reasonably well. The results of the sensitivity test of initial conditions showed that when the intensity of the upper-level trough in the initial time was strengthened, the high-pressure zone would break ahead of time, leading to early northward turning of Morakot. Conversely, when the intensity was weakened, the breaking of the high-pressure zone would be delayed. Especially, when the intensity was weakened to a certain extent, the high-pressure zone would not break. The typhoon, steered by the easterly flow to the south of the high-pressure zone, would keep moving westward, with no turning in the test.

(3) The diagnostic analysis of the physical fields based on the results of sensitivity test revealed that the

positive vorticity advection and cold advection associated with the upper-level trough weaken the intensity of the high-pressure zone; the existence of the upper-level trough was the main leading factor for the breaking of the high-pressure zone. The upper-level trough affected typhoon's track indirectly by influencing the high-pressure zone, suggesting that when making forecasting, one should not only pay attention to the synoptic weather systems around the typhoon, but should also be concerned with some possible indirect effects—a new clue in the typhoon prediction—imposed from other systems.

In addition, the diagnostic analysis in this work indicated that Morakot might also play a role in the split of the high-pressure zone and thus affected its own track. There is a growing interest in the study of the interaction between the typhoon and the subtropical high, which needs to be examined in the future.

REFERENCES:

- [1] CHEN Lian-shou, XU Xiang-de, LUO Zhe-xian. An introduction to tropical cyclone dynamic [M]. Beijing: China Meteorological Press, 2002: 316pp (in Chinese).
- [2] ZHANG Sheng-jun, CHEN Lian-shou, XU Xiang-de. The diagnoses and numerical simulation on the unusual track of Helen (9505) [J]. Chin. J. Atmos. Sci., 2005, 29(6): 937-946 (in Chinese).
- [3] FAN Jun-hong, LI Yun-chuan, CHEN Xiao-lei, et al. The analysis of track turning eastward of typhoon Matsa and the test of NWP [J]. Sci. Meteor. Sinica, 2007, 27(S1): 134-139 (in Chinese).
- [4] XU Jing, CHEN Lian-shou, XU Xiang-de. Diagnosis of the

impact of middle troposphere circulation pattern over the Qinghai-Xizang plateau on the track of typhoon over west Pacific [J]. *Quart. J. Appl. Meteor.*, 1999, 10(4): 410-420 (in Chinese).

[5] HOSKINS B J, MCINTYRE M E, ROBERTSON A. On the use and significance of isentropic potential vorticity maps [J]. *Quart. J. Roy. Meteor. Soc.*, 1985, 111(470): 877-946.

[6] DAVIS C A, EMANUEL K A. Potential vorticity diagnostics of cyclogenesis [J]. *Mon. Wea. Rev.*, 1991, 119(8): 1929-1953.

[7] WU C C, EMANUEL K A. Potential vorticity diagnostics of hurricane movement. Part I: A case study of Hurricane Bob (1991) [J]. *Mon. Wea. Rev.*, 1995, 123(1): 69-92.

[8] WU C C, EMANUEL K A. Potential vorticity diagnostics of hurricane movement. Part II: Tropical storm Ana (1991) and Hurricane Andrew (1992) [J]. *Mon. Wea. Rev.*, 1995, 123(1): 93-109.

[9] WU C C, HUANG T S, CHOU K H. Potential vorticity diagnosis of the key factors affection the motion of Typhoon Sinlaku (2002) [J]. *Mon. Wea. Rev.*, 2004, 132(8): 2084-2093.

[10] JI Liang. The numerical simulation of the effect of mid-latitude and subtropical systems on landfall tropical cyclone [D]. Ph.D. dissertation, 2007 (in Chinese).

[11] JI Liang, FEI Jian-fang, HUANG Xiao-gang. Numerical simulation of the effect of the subtropical high on landfalling tropical cyclones [J]. *Acta Meteor. Sinica*, 2010, 68(1): 40-47 (in Chinese).

[12] ZHANG Da-lin, KIEU C Q. Potential vorticity diagnosis of a simulated hurricane. Part II: Quasi-balanced contributions to forced secondary circulations [J]. *J Atmos. Sci.*, 2006, 63(11): 2898-2914.

[13] WANG Xing-bao, ZHANG Da-lin. Potential vorticity diagnosis of a simulated hurricane. Part I: Formulation and quasi-balanced flow [J]. *J. Atmos. Sci.*, 2003, 60(13): 1593-1607.

[14] KIEU C Q, ZHANG Da-lin. A piecewise potential vorticity inversion algorithm and its application to hurricane inner-core anomalies [J]. *J. Atmos. Sci.*, 2010, 67(8): 2616-2631.

[15] ARTHUR C P. Geopotential heights and thicknesses as predictors of Atlantic tropical cyclone motion and intensity [J]. *Mon. Wea. Rev.*, 1985, 113(6): 931-939.

[16] An online poster. How to predict tropical cyclones with the aid of steering airflows? (in Chinese) [EB/OL]. [2011-09-30] <http://tieba.baidu.com/f?kz=259043629>.

Citation: FEI Jian-fang, LI Bo, HUANG Xiao-gang et al. On the relationships between the unusual track of typhoon Morakot (0908) and the upper westerly trough. *J. Trop. Meteor.*, 2012, 18(2): 187-194.